Electronic Supplementary Material (ESI) for Nanoscale.
This journal is © The Royal Society of Chemistry 2018

Fluctuating potentials in GaAs:Si nanowires: critical reduction of the influence of polytypism on the electronic structure

N. Ben Sedrine,*[a] R. Ribeiro-Andrade,[b,f] A. Gustafsson,[c] M. R. Soares,[d] J. Bourgard,[a] J. P. Teixeira,[a] P. M. P. Salomé,[b,e] M. R. Correia,[a] M. V. B. Moreira,[f] A. G. De Oliveira,[f] J. C. González,[f] and J. P. Leitão[a]

[a.] *Departamento de Física and I3N, Universidade de Aveiro, Campus Universitário de Santiago, 3810-193 Aveiro, Portugal*
[b.] *INL - International Iberian Nanotechnology Laboratory, Quantitative Electron Microscopy, Avenida Mestre José Veiga, 4715-330 Braga, Portugal*
[c.] *Solid State Physics and NanoLund, Box 118, Lund University, Lund SE-22100, Sweden*
[d.] *Laboratório Central de Análises, Universidade de Aveiro, 3810-193 Aveiro, Portugal*
[e.] *Departamento de Física, Universidade de Aveiro, Campus Universitário de Santiago, 3810-193 Aveiro, Portugal*
[f.] *Departamento de Física, Universidade Federal de Minas Gerais, 30123-970 Belo Horizonte, Minas Gerais, Brazil*

Effect of the epilayer on the luminescence

We first verified that the GaAs epilayer grown beneath the NWs was not observed in the luminescence, since no signal was detected when the laser spot was outside the NWs growth region. This result is in accordance with our previous report[2]. Indeed, Fig. SI1 shows the luminescence measured by cathodoluminescence (CL) when the electron beam is focused outside the NWs ensemble in sample B (green curve), i.e. in the GaAs epilayer grown on top of the substrate. In this case, a broad and asymmetric band is observed at higher energies (~1.44 - 1.62 eV) than the luminescence from the NWs in sample B (red curve), indicating a possible Burstein-Moss shift effect in the epilayer. The luminescence from the NWs in sample A is also shown for comparison. Thus, one can conclude that no significant influence of the epilayer exist on the NW's luminescence.

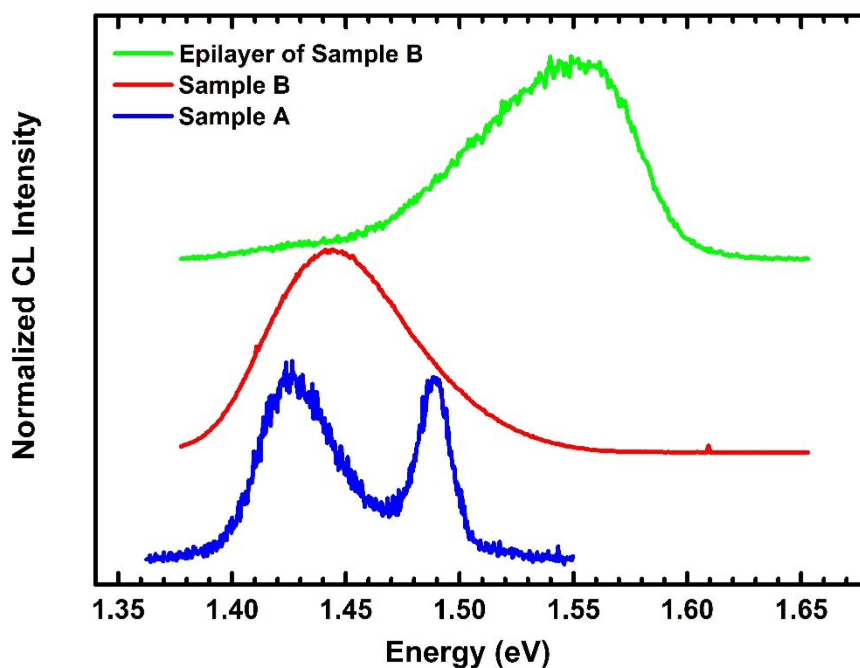

Fig. SI1: Normalized CL spectra measured at 8 K of Si-doped GaAs NW ensemble in samples A and B. The used accelerating voltage is 5 kV, while the used current is 25 pA for sample A, and 20 pA for sample B and corresponding epilayer.

SEM Characterization

Scanning electron microscopy (SEM) was carried out with a high performance Schottky field emission HR-FESEM Hitachi SU-70 microscope equipped with in-lens secondary-electron and backscattered-electron detectors.

Representative SEM micrograph images of the nanowires (NWs) of all samples are illustrated in Fig. SI2 for the cross section (a and c) and top view (b and d) of sample A. Fig. SI2 (a) evidences that the growth of the GaAs NWs on GaAs (111)B substrate produces dense and different orientations of the NWs. The dominant orientation of the short NWs is slightly vertical, suggesting an epitaxial relationship with the substrate[1]. The NW lengths reach up to several tens of micrometers and their diameters vary along the axis from a few hundreds of nanometers at the base to a few tens of nanometers at the tip. The orientation, dimensions and shape of NWs are in accordance with our previous reports[2,3] suggesting a negligible influence of either: the chemical nature of the impurity (Si in the present work and Mg in Refs. 2,3) or the doping level on the morphological properties of the NWs ensemble. These findings are in accordance with the literature[4]. Although it was reported that the presence of dopant atoms in vapour phase may change the morphology of NWs such as doping with Te[5] that causes an increase in radial growth of GaAs NWs due to its surfactant effects, our findings are in good agreement with Hilse *et al*.[6] who demonstrated that the Si concentration did not affect the shape of the GaAs NWs grown on Si(111) substrates by molecular beam epitaxy based on the vapor-liquid-solid mechanism.

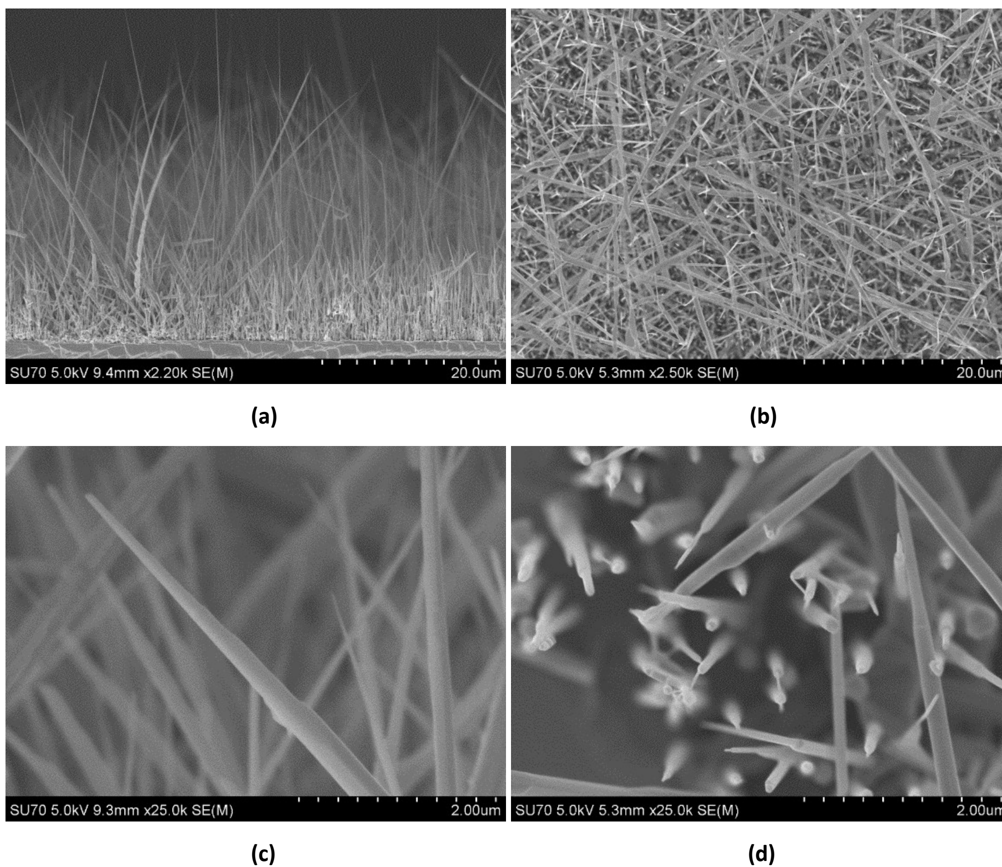

Fig. SI2: Representative SEM images of the Si-doped GaAs NWs; sample A: cross section (a and c) and top view (b and d).

Structural characterization: TEM

For the present study, more than ten NWs from samples A and B were investigated with TEM. Representative TEM images of two single Si-doped GaAs NWs were selected in Figures 4 (a), (b). In the following Fig. SI3, we present additional TEM images for two more nanowires for each sample. It can be clearly seen that a similar structure is found for the present NWs when compared to the ones in Figures 4 (a), (b), corroborating with the general trend of all the NWs, which exhibit a mixture of ZB and WZ segments as well as twinned ZB segments along the NW axis.

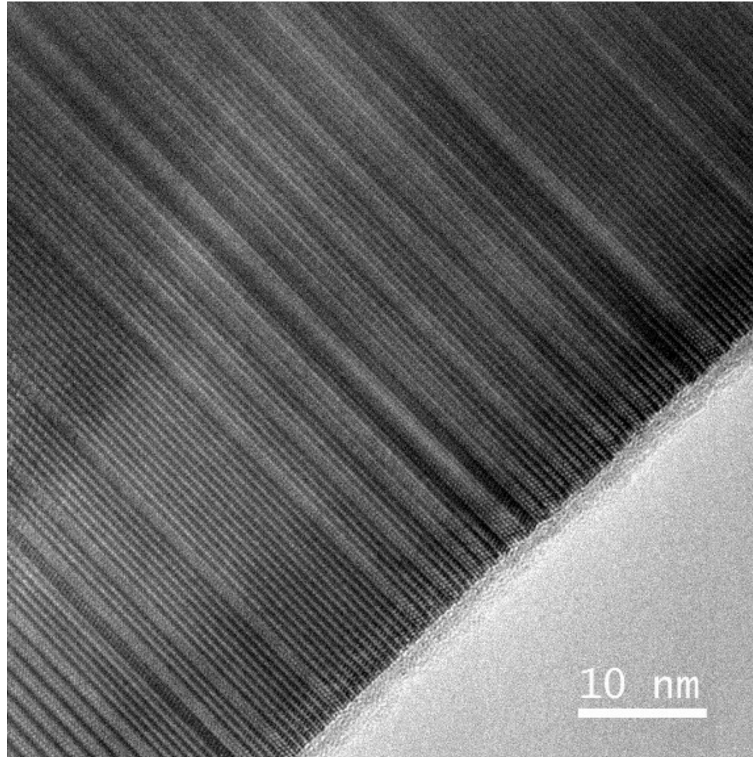

(a)

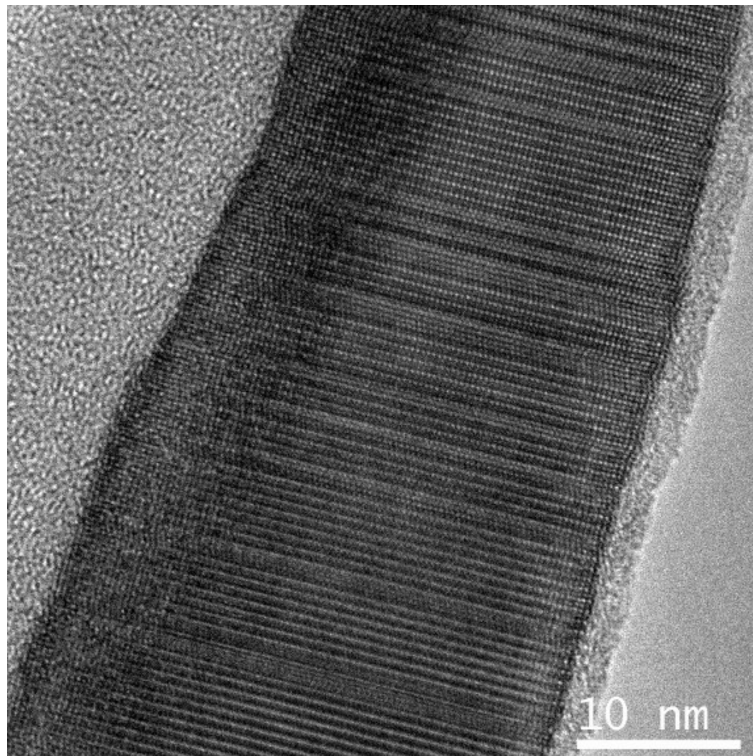

(b)

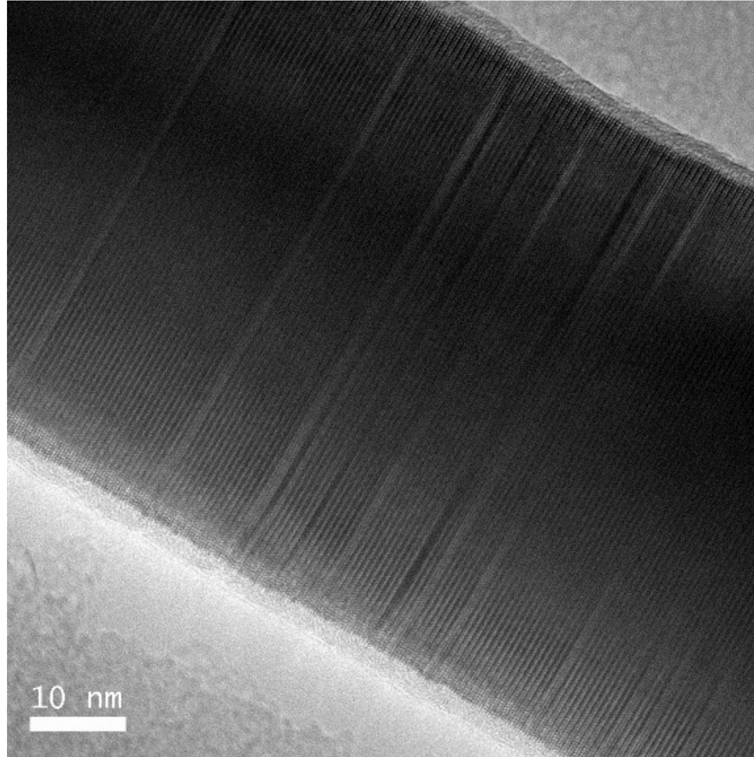

(c)

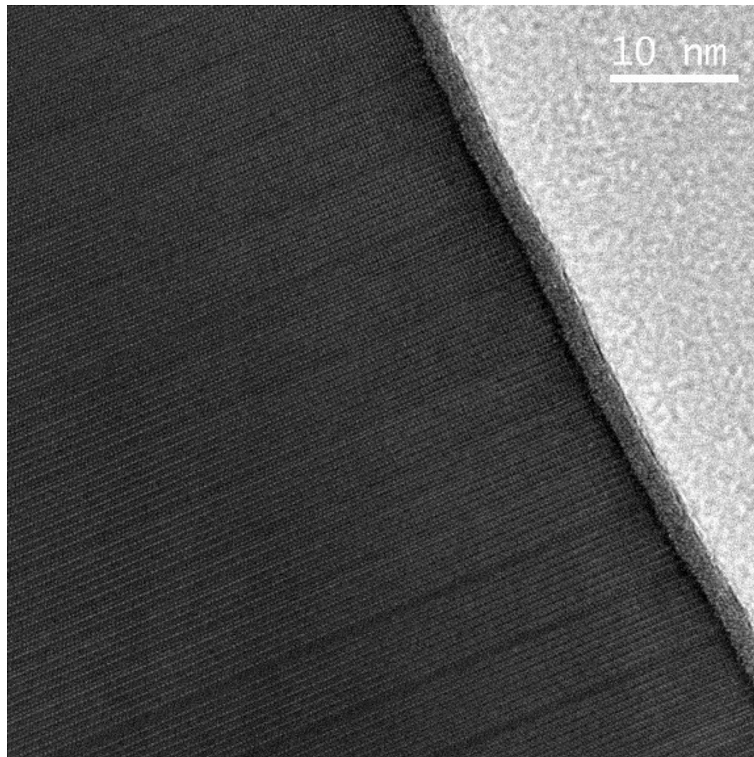

(d)

Fig. SI3: TEM images of two single Si-doped GaAs NWs, different from the ones shown in Fig. 4, for sample A (a and b) and sample B (c and d).

Deconvolution of the PL spectra

The typical PL spectra, measured at 5 K under excitation power of 100 mW and 2 mW for the samples A and B, respectively, are illustrated in Fig. SI4. The deconvolution method consists on the decomposition into the minimum number of Gaussian components (four in our case) necessary to best describe the experimental PL spectra (in black). In both cases, the baseline was described by a fifth Gaussian component with a high FWHM. For sample A, the deconvolution was performed in the energy range of the most intense luminescence, 1.38-1.50 eV, where the four components (A_1, A_2, A_3 and A_4) are interpreted as independent radiative transitions. For sample B, a broader energy range was assumed since the luminescence is broader. In such case, the set of all measured PL spectra evidences that the luminescence corresponds to two broad transitions: *i)* a dominant and asymmetric one centred at ~1.42 eV (denoted by B') and fitted by three components B_1, B_2 and B_3, *ii)* a second transition above ~1.45 eV, described by a component B_4 (also denoted by B_4). It should be noticed that the asymmetry of the dominant transition B' is approximatively independent of excitation power and temperature in all the PL spectra. Therefore for sample B, our PL spectra are interpreted in terms of two radiative transitions B' and B_4. Similar deconvolution procedures were performed for the samples A* and B*.

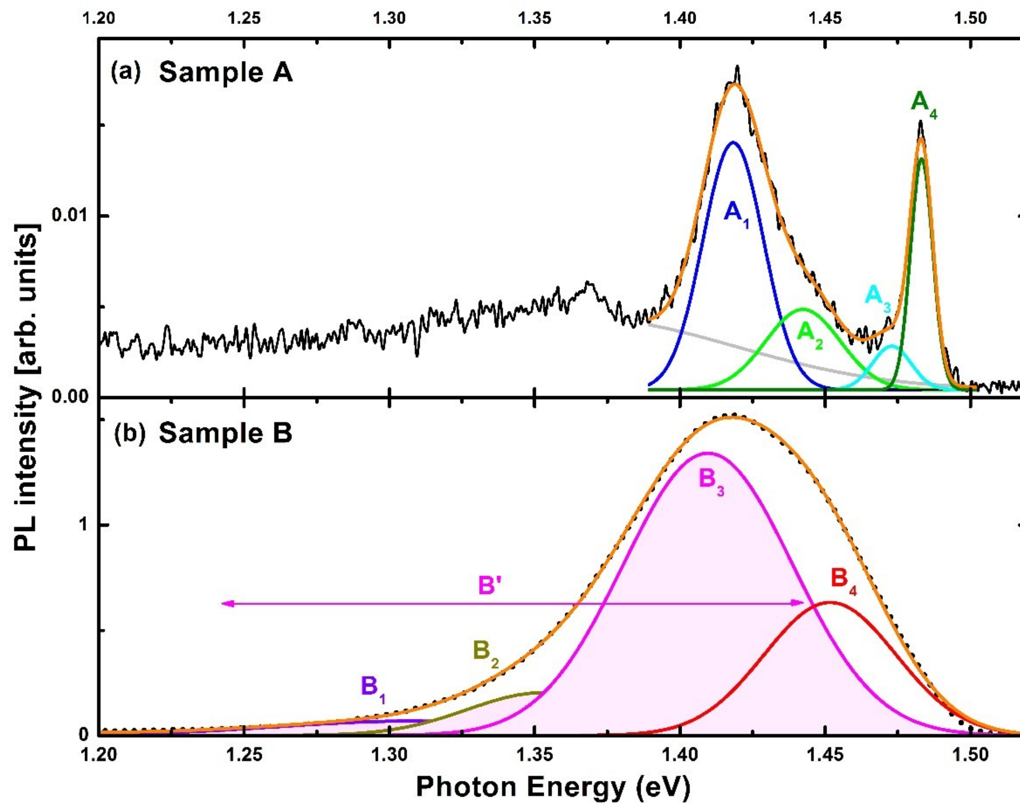

Fig. SI4: PL spectra (in black) measured at 5 K of Si-doped GaAs NW ensemble for samples A at 100 mW (a) and B at 2 mW (b). The best-fit model using Gaussian components is shown for both samples (orange lines).
The different components A_i and B_i (i=1,2,3,4) are also identified for each sample. In the case of sample B, the three components B_1, B_2, B_3 define the dominant radiative transition (B') observed for lower energies. The arrow highlights roughly the spectral region where the B' transition is dominant.

Dependence on the excitation power:

Fig. SI5 (a), (b) represent the dependence on the excitation power of the relative intensity of the radiative transitions as well as the radiative transition peak energy of Si-doped GaAs NW ensembles for samples A, A*, B and B* (with nominal free carrier concentrations of $1x10^{16}$, $8x10^{16}$, $1x10^{18}$ and $5x10^{18}$ cm^{-3}, respectively), measured at 5 K. Solid lines in Fig. SI5 (a) represent the fit of Eq. (1) to each set of the experimental points. The obtained best-fit values of the *m* parameters are: 0.56 $\pm$ 0.02, 0.44 $\pm$ 0.02, and 0.57 $\pm$ 0.02, respectively for the components A^*_1, A^*_2 and A^*_3 of sample A*, and 0.85 $\pm$ 0.01 for the component B*' of sample B*. Solid lines in Fig. SI5 (b) represent the best-fit using eq. (2), and the obtained best-fit β values (in meV) are: 0.20 $\pm$ 0.02, 0.20 $\pm$ 0.06, and 0, for the components A^*_1, A^*_2 and A^*_3, respectively for sample A*, and 7.8 $\pm$ 0.2 for the component B*' for sample B*. These results clearly show that the samples can be dissociated into two sets: a) samples A and A^*; b) samples B and B^*.

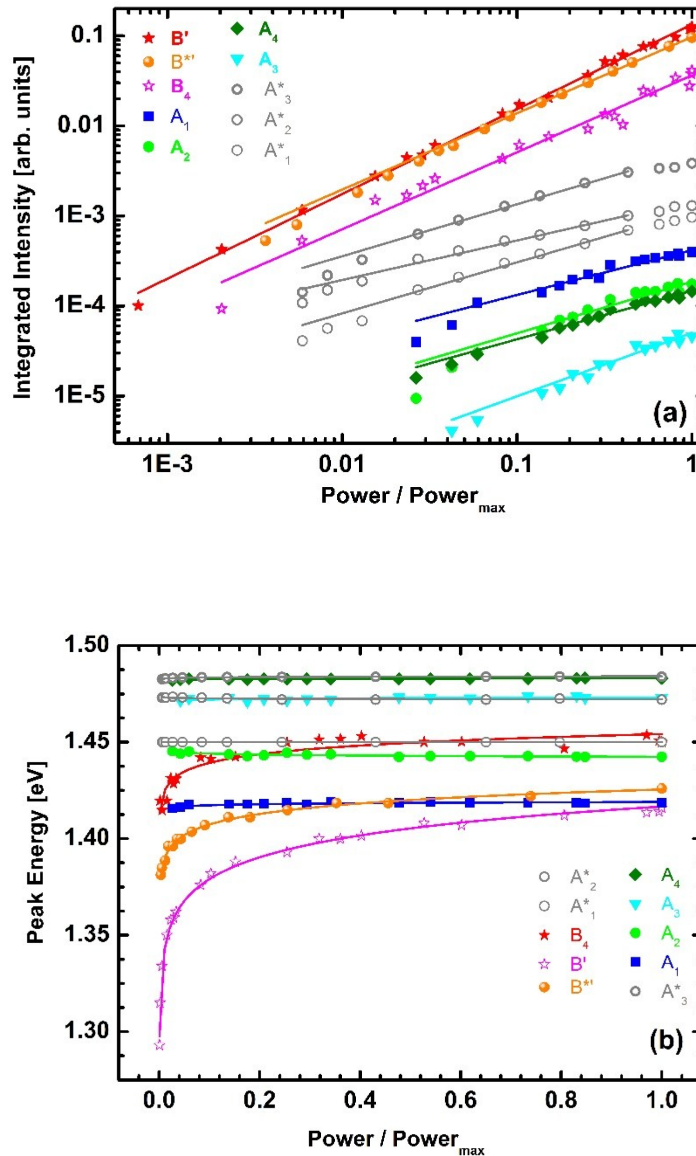

Fig. SI5: (a) Dependence on the excitation power of the relative intensity of the radiative transitions in Si-doped GaAs NW ensembles for samples A, A*, B and B*, measured at 5 K. The lines represent the fit of Eq. (1) to each set of experimental points. (b) Dependence on the excitation power *P* of the radiative transition peak energy of the Si-doped GaAs NW ensemble for samples A, A*, B and B*. Solid lines represent the best-fit using eq. (2).

Dependence on the excitation power for Sample B:

Fig. SI6 demonstrates that, in the case of sample B, the blue-shift cannot be related to a change of the relative intensities of the different transitions. Indeed, the Gaussian components B' (magenta) and B_4 (red) clearly evidence a blue-shift when increasing the excitation power.

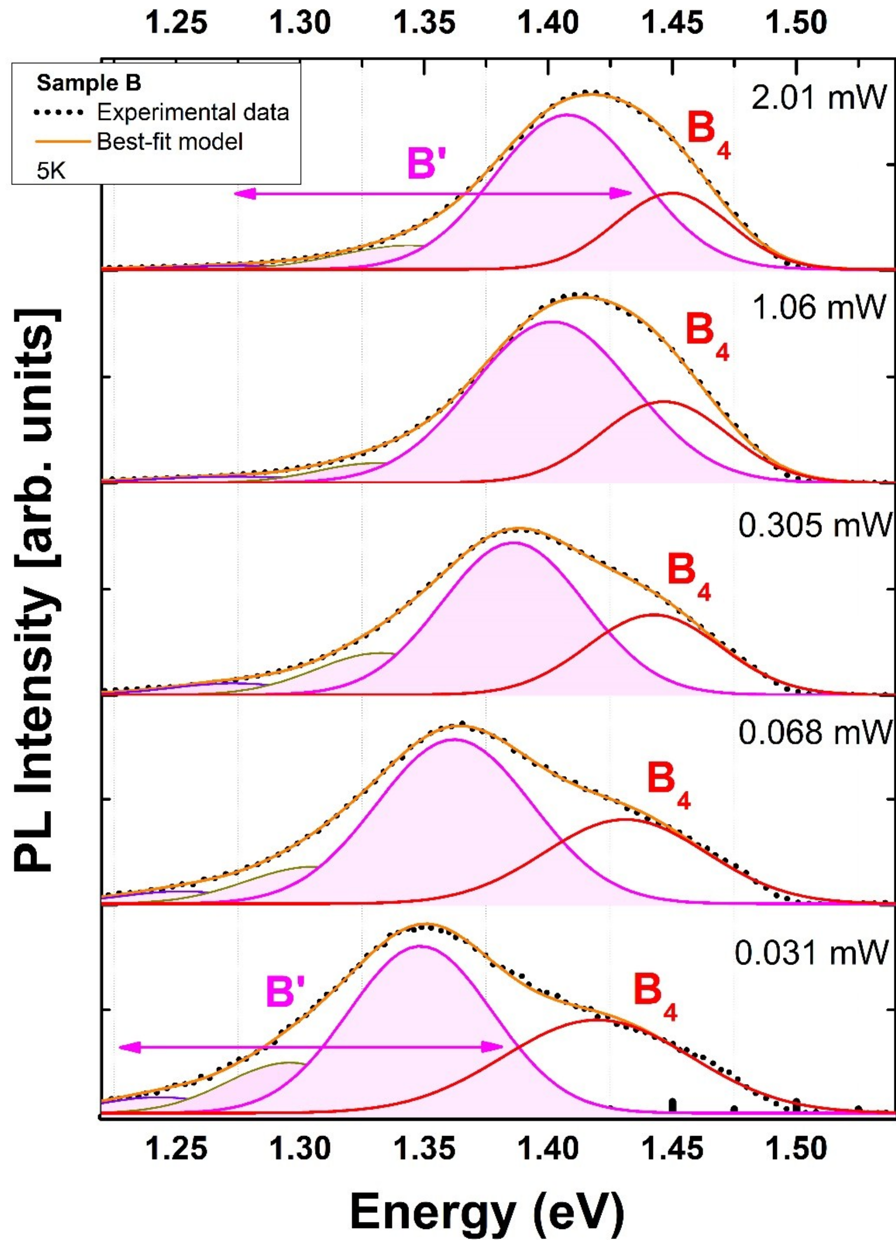

Fig. SI6: PL spectra (black dotted lines) measured at 5 K of Si-doped GaAs NW ensemble for sample B at different excitation power values. The best-fit model using Gaussian components is shown (orange lines). The components B_3 (magenta) and B_4 (red) clearly indicate the blue-shift when increasing the excitation power. The arrows highlight roughly the spectral regions for two PL spectra where the B' transition is dominant.

Estimation of the depth of the fluctuating potentials for sample B*:

Fig. SI7 shows the fit with eq. (5) to the low energy side of the PL spectrum measured at low temperature for sample B^*.

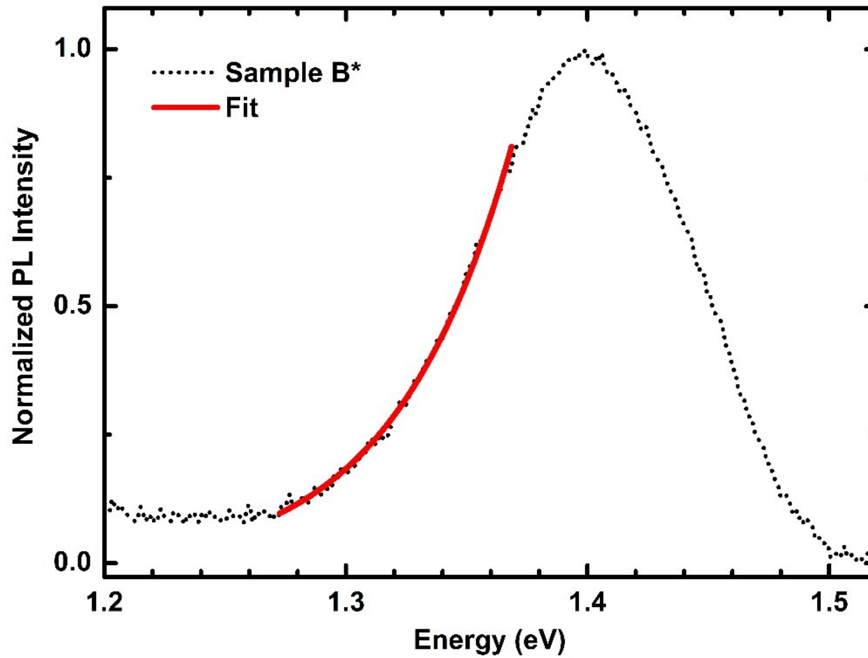

Fig. SI7: Estimation of the depth of the fluctuating potentials for sample B* using eq. (5), γ = 117.3 ± 0.4 meV; the fit is realized for the PL spectrum measured at 5 K (presented in Fig. 1), in the range 1.31–1.39 eV.

[1] E. Uccelli, J. Arbiol, C. Magen, P. Krogstrup, E. Russo-Averchi, M. Heiss, G. Mugny, F. Morier-Genoud, J. Nygard, J. R. Morante and A. Fontcuberta I Morral, *Nano Lett.*, 2011, **11**, 3827.

[2] B. P. Falcão, J. P. Leitão, M. R. Correia, M. R. Soares, F. M. Morales, J. M. Mánuel, R. Garcia, A. Gustafsson, M. V. B. Moreira, A. G. De Oliveira and J. C. González, *J. Appl. Phys.*, 2013, **114**, 183508.

[3] P. Kannappan, N. Ben Sedrine, J. P. Teixeira, M. R. Soares, B. P. Falcão, M. R. Correia, N. Cifuentes, E. R. Viana, M. V. B. Moreira, G. M. Ribeiro, A. G. de Oliveira, J. C. González, and J. P. Leitão, Substrate and Mg doping effects in GaAs nanowires, *Beilstein J. Nanotechnol.*, 2017, **8**, 2126.

[4] M. Heiss, S. Conesa-Boj, J. Ren, H. H. Tseng, A. Gali, A. Rudolph, E. Uccelli, F. Peiro, J. R. Morante, D. Schuh, E. Reiger, E. Kaxiras, J. Arbiol and A. Fontcuberta I Morral, *Phys. Rev. B - Condens. Matter Mater. Phys.*, 2011, **83**, 1.

[5] J. A. Czaban, D. A. Thompson and R. R. LaPierre, *Nano Lett.*, 2008, **9**, 148.

[6] M. Hilse, M. Ramsteiner, S. Breuer, L. Geelhaar and H. Riechert, *Appl. Phys. Lett.*, 2010, **96**, 10.